



Vibrational Spectroscopic Investigation on Bisthiourea Magnesium Sulphate (BTMS) Using Experimental and Computational [HF and DFT] Analysis

Durga R¹, Anand S^{1*}, Sundararajan RS² and Ramachandraraja C²

¹Department of Physics, AVC College, Mayiladuthurai, Tamil Nadu, India

²Department of Physics, Government Arts College, Kumbakonam, Tamil Nadu, India

Abstract

Nonlinear optical bisthiourea mixed magnesium sulphate BTMS crystals were synthesized and grown by slow evaporation method using water as solvent. Vibrational spectra were recorded to determine the symmetries of molecular vibrations. These observations suggest that the metals coordinate with thiourea through sulphur. The observed peaks IR and Raman were assigned according to their distinctiveness region. The hybrid computational calculations were carried out for calculating geometrical and vibrational parameters by HF and DFT methods with basis sets and the corresponding results were tabulated. UV-Vis-NIR spectra were recorded to study the optical transparency of the grown crystals. The observed Raman and infrared bands were also assigned and discussed. The optical transmission spectral study was carried out to test the transmitting ability of the crystal in the visible range. The second harmonic generation test of BTMS revealed the nonlinear nature of the crystal. The TGA/DTA curve was also recorded for the experimental crystal. The lattice parameters of the grown crystal have been determined by X-ray diffraction studies.

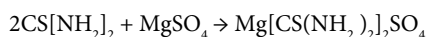
Keywords: BTMS; SHG; NLO activity; FMO; Optical properties; Hybrid Gaussian

Introduction

Nonlinear optical (NLO) Materials play an important role in nonlinear optics, optical communication, optical switching, optical disk data storage, laser fusion reactions, optical rectifications and in particular they have a great impact on information technology and industrial applications [1-6]. The approach of combining the high nonlinear optical coefficient of the organic molecules with the excellent physical properties of the inorganics found to be extremely successful in the recent past. Thiourea, which is centrosymmetric, yields excellent non centrosymmetric materials. These materials are formed by combining organic molecules of high polarizability with thermally stable and mechanically robust inorganic molecules. These materials in addition to retaining high optical nonlinearities of organic molecules also possess favourable physical properties. An added advantage is that large single crystals can be grown from slow evaporation solution growth [7,8]. The literature survey reveals that, to the best of our knowledge, no intensive observation of spectroscopic [FT-IR and FT-Raman] and theoretical [HF/DFT] investigation has been reported so far.

Experimental Methods

BTMS crystal was synthesized by dissolving AR grade thiourea and AR grade magnesium sulphate in the molar ratio 2:1 in distilled water. The saturated solution of magnesium sulphate is slowly added to the saturated solution of thiourea. This is stirred well to get a clear solution. Pure BTMS crystal was synthesized according to the reaction:



The solution was purified by repeated filtration. The saturated solution was kept in a beaker covered with polythene paper. For slow evaporation 6 or 7 holes are made in the polythene paper. Then the solution is left undisturbed in a constant temperature bath (CTB) kept at a temperature of 35°C with an accuracy of $\pm 0.1^\circ\text{C}$. As a result of slow evaporation, after 75 days colourless and transparent pure BTMS crystals were obtained (Figure 1).

The FT-IR spectrum of the compound is recorded in Bruker IFS 66V spectrometer in the range of 4000-100 cm^{-1} . The spectral resolution is $\pm 2 \text{ cm}^{-1}$. The FT-Raman spectrum of AMS is also recorded in the same instrument with FRA 106 Raman module equipped with Nd:YAG laser source operating at 1.064 μm line widths with 200 mW power. The spectra are recorded in the range of 4000-100 cm^{-1} with scanning speed of 30 $\text{cm}^{-1} \text{ min}^{-1}$ of spectral width 2 cm^{-1} . The frequencies of all sharp bands are accurate to $\pm 1 \text{ cm}^{-1}$. The transmission spectrum of BTMS was recorded using Varion Cary 5E UV-Vis-NIR Spectro photometer. The Thermogravimetric analysis and Differential thermal analysis (TGA and DTA) curves for BTMS were obtained using Simultaneous Thermogravimetric Analyser (STA) 409 C (NET- ZSCH) made in Germany at a heating rate of 10 $^\circ\text{C}/\text{min}$ in Nitrogen. The single crystals of BTMS have been subjected to X-ray diffraction studies using an ENRAF NONIUS CAD4 X-ray diffractometer.

Computational Methods

In the present work, some of the hybrid methods such as HF and DFT, were carried out using the basis sets 6-311+G(d,p) and 6-311++G(d,p). All these calculations were performed using GAUSSIAN 09W program package on Pentium core i3 processor in personal computer. In DFT methods; Becke's three parameter hybrids function combined with the Lee-Yang-Parr correlation function (B3LYP), Becke's three parameter exact exchange-functions (B3) combined with gradient-corrected

***Corresponding author:** Anand S, Department of Physics, AVC College, Mayiladuthurai, Tamil Nadu, India, Tel: +919443650530; E-mail: anandphy09@gmail.com

Received February 17, 2017; Accepted March 29, 2017; Published April 05, 2017

Citation: Durga R, Anand S, Sundararajan RS, Ramachandraraja C (2017) Vibrational Spectroscopic Investigation on Bisthiourea Magnesium Sulphate (BTMS) Using Experimental and Computational [HF and DFT] Analysis. J Theor Comput Sci 4: 153. doi:10.4172/2376-130X.1000153

Copyright: © 2017 Durga R, et al. This is an open-access article distributed under the terms of the Creative Commons Attribution License, which permits unrestricted use, distribution, and reproduction in any medium, provided the original author and source are credited.

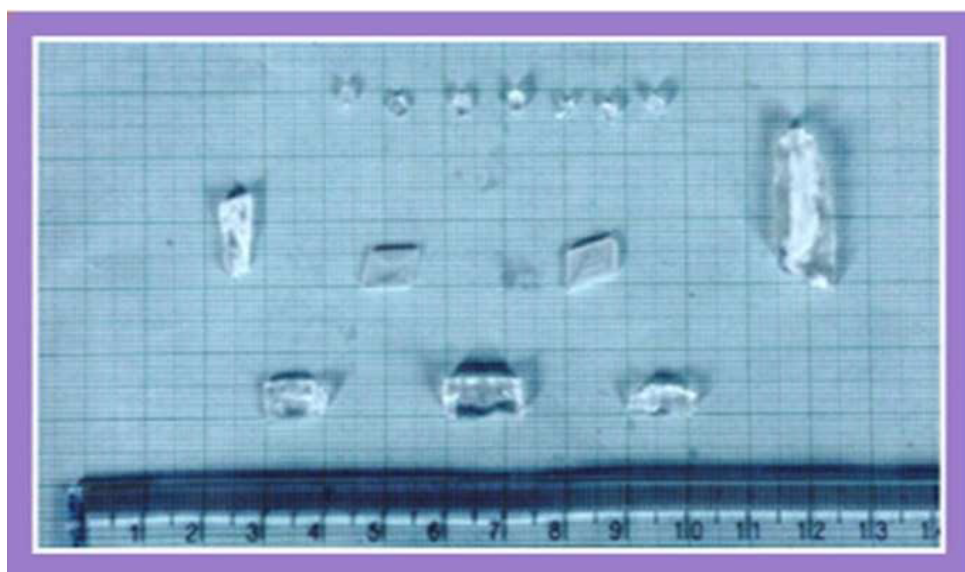


Figure 1: Photograph of grown BTMS crystals.

correlation functional of Lee, Yang and Parr (LYP). The optimized structural parameters are used in the vibrational frequency calculations at DFT (B3LYP) levels. The minimum energy of geometrical structure is obtained by using level 6-31++G(d,p) and 6-311++G(d,p) basis sets. At the optimized geometry for the title molecule no imaginary frequency modes are obtained, so there is a true minimum on the potential energy surface is found. The calculated frequencies are scaled by 0.85, 0.88, 0.95, 0.98 and 1.25 for HF/6-31++/6-311++G(d,p), B3LYP/631++/6-311++G(d,p) and B3PW91/6-31++G(d,p) method basis set. The electronic properties, such as HOMO-LUMO energies, absorption wavelengths and oscillator strengths are calculated using B3LYP method of the time-dependent DFT (TD-DFT), based on the optimized structure in solvent (DMSO, chloroform and CCl_4) and gas phase. The thermodynamic properties of the title compound at different temperatures have been calculated in gas phase using B3LYP/6-311++G (d,p) method. The observed (FT-IR and FT-Raman) and calculated vibrational frequencies and vibrational assignments are submitted in Table 1. Experimental and simulated spectra of IR and Raman are presented in the Figures 2 and 3, respectively.

Results and Discussion

Molecular geometry

The molecular structure of BTMS belongs to C_s point group symmetry. The optimized molecular structure of the molecule is obtained from Gaussian 09 and Gauss view program and is shown in Figure 4. The molecule contains two thiourea group connected with MgSO_4 . The structure optimization and zero point vibrational energy of the compound in HF/DFT-B3LYP/6-31++G(d,p) and 6-311++G(d,p) are 96.88, 89.80 and 89.81 Kcal/Mol respectively. The comparative optimized structural parameters such as bond lengths, bond angles and dihedral angles are presented in Table 1.

The molecular structure is optimized by Berny's optimization algorithm using Gaussian 09 and Gauss view program and is shown in Figure 4. The comparative optimized structural parameters such as bond length, bond angle and dihedral angle are presented in Table 2. The present compound contains magnesium as a metal atom, sulphate

atoms and four amino groups. The calculated energy of HF is greater than DFT method because the assumption of ground state energy in HF is greater than the true energy. Though, the molecular structure belongs to one plane, with respect to magnesium the thiourea on both sides are somewhat tilted due to attraction between Mg and H.

The experimental bond length of C-S and C-N are 1.720 and 1.340Å whereas the calculated bond lengths are 1.736 and 1.329 Å respectively. Though, both the amino groups are coupled with carbon symmetrically, the bond distance of C-N is differed by 0.016 Å between them due to the attraction of H by Mg. Normally, the double bond is to be there between C and S atoms, but one bond alone is there due to 2 lone pair of electrons are transferred from ligand to metal. The calculated bond length of Mg-S is 2.488 Å which is long and strong van der Waals bond. The internuclear distance of N5-H6 and N8-H9 are same and are 0.015 Å higher than other N-H bonds due to the existence of Mg and H attraction. From the optimized parameters, it is inferred that, the organo-metallic compound is very strong due to the complex bonds.

Vibrational assignments

The BTMS molecule consists of 22 atoms, which undergoes 60 normal modes of vibrations. On the assumption of C_s group of symmetries, the numbers of vibration modes of the 60 fundamental vibrations of the molecule can be distributed as

$$\Gamma_{\text{vib}} = 36 A' + 24 A''$$

In accordance with the C_s group symmetry, all the 60 fundamental vibrations are to be active both in Raman and IR. However the intensity of certain peaks is so weak, they are found missing in the spectra, which can be verified from the intensity values calculated theoretically. The calculated (scaled) and experimental frequency values, for different methods and basis sets and the corresponding assignments are presented in the Table 1. The unscaled values of frequencies are presented in Table 3. The equivalent FT-IR and FT-Raman spectra were described in Figures 2 and 3 respectively. All the observed bands are assigned to different possible modes of vibrations based on the earlier works on structurally similar molecules, the characteristic frequencies

S. No	Symmetry Species C_s	Observed Frequency (cm ⁻¹)		Methods					Vibrational Assignments
				HF		B3LYP		B3PW91	
				6-31++G (d-p)	6-311++G (d-p)	6-31++G (d-p)	6-311++G (d-p)	6-31++G (d-p)	
FT- IR	FT- Raman								
1	A'	3773 w	-	3771	3771	3771	3758	3768	(N-H) ν
2	A'	3755 w	-	3731	3751	3742	3720	3730	(N-H) ν
3	A'	-	3381 s	3375	3395	3374	3358	3363	(N-H) ν
4	A'	-	3296 s	3297	3278	3265	3278	3290	(N-H) ν
5	A'	3277 s	-	3254	3241	3278	3267	3264	(N-H) ν
6	A'	-	3192 s	3178	3203	3170	3193	3191	(N-H) ν
7	A'	3179 s	-	3167	3158	3142	3177	3170	(N-H) ν
8	A'	2715 w	-	2692	2689	2719	2722	2719	(N=C=N) ν
9	A'	2143 w	-	2135	2132	2137	2141	2138	(N=C=N) ν
10	A'	2048 w	-	2040	2037	2047	2036	2050	(N=C=N) ν
11	A'	1836 w	-	1805	1832	1829	1820	1835	(N=C=N) ν
12	A'	-	1645 s	1623	1634	1628	1652	1668	(N-H) δ
13	A'	1618 s	-	1603	1610	1606	1610	1617	(N-H) δ
14	A'	1518 s	-	1517	1507	1510	1546	1546	(N-H) δ
15	A'	-	1492 s	1489	1481	1477	1478	1487	(N-H) δ
16	A'	1473 s	-	1469	1461	1472	1462	1466	(N-H) δ
17	A'	1412 vs	-	1390	1389	1410	1407	1411	(S=O) ν
18	A''	-	1393 vs	1383	1379	1389	1386	1390	(S=O) ν
19	A''	-	1105 s	1105	1101	1102	1113	1107	(N-H) δ
20	A'	1098 s	-	1093	1089	1089	1087	1096	(N-H) δ
21	A'	1083 s	-	1081	1079	1081	1078	1080	(N-H) δ
22	A'	1061 s	-	1057	1055	1080	1051	1058	(C-N) ν
23	A'	998 m	-	1016	1005	988	990	992	(C-N) ν
24	A'	960 m	-	997	960	952	954	955	(N-H) γ
25	A'	845 m	-	836	849	843	843	863	(N-H) γ
26	A''	-	746 m	744	741	738	740	741	(C-N) ν
27	A''	730 m	-	725	725	711	714	723	(C-N) ν
28	A''	715 m	-	715	714	705	706	718	(N-H) γ
29	A''	643 w	-	640	640	656	652	660	(N-H) γ
30	A''	625 w	-	626	620	623	644	620	(N-H) γ
31	A''	613 w	-	617	612	612	610	613	(N-H) γ
32	A'	590 w	-	587	583	576	580	583	(N-H) γ
33	A'	550 w	-	549	547	564	566	570	(N-H) γ
34	A'	545 w	-	540	541	552	555	555	(N-H) γ
35	A''	520 w	-	516	516	517	545	520	(N-H) γ
36	A''	510 w	-	505	506	509	536	511	(C-N) δ
37	A''	485 w	-	481	483	487	488	491	(C-N) δ
38	A'	470 w	-	467	467	480	468	483	(C-S) δ
39	A''	440 w	-	438	438	439	440	442	(C-S) δ
40	A''	435 w	-	430	432	438	433	441	(Mg-O (S)) ν
41	A''	425 w	-	425	422	433	427	437	(Mg-O (S)) ν

42	A ⁻	422 w	-	421	417	432	423	434	(Mg-O-S) δ
43	A ⁻	390 w	-	416	386	403	410	406	(Mg-O-S) δ
44	A ⁻	340 w	-	341	337	338	336	338	(Mg-O-S) γ
45	A ⁺	250 w	-	249	248	246	248	246	(Mg-O-S) γ
46	A ⁺	240 w	-	237	237	238	238	239	(Mg-O-S) γ
47	A ⁺	230 w	-	229	229	228	237	230	(C-N) δ
48	A ⁺	210 w	-	214	207	208	226	209	(C-N) δ
49	A ⁺	200 w	-	212	198	207	211	208	(C-N) γ
50	A ⁺	190 w	-	192	188	200	195	201	(C-N) γ
51	A ⁻	180 w	-	171	174	181	175	182	(C-S) γ
52	A ⁻	160 w	-	169	172	168	155	166	(C-S) γ
53	A ⁻	155 w	-	123	123	119	118	117	(C-N) γ
54	A ⁻	150 w	-	108	107	114	109	114	(C-N) γ
55	A ⁻	140 w	-	105	104	112	99	111	(C-S) γ
56	A ⁻	130 w	-	86	87	86	82	85	(C-S) γ
57	A ⁻	120 w	-	59	56	54	63	54	(C-N) γ
58	A ⁺	110 w	-	53	52	51	54	50	(C-S) γ
59	A ⁺	105 w	-	30	25	33	33	33	(C-S) γ
60	A ⁻	100 w	-	23	21	22	21	22	(C-S) γ

Note: s – Strong; m- Medium; w – weak; as- Asymmetric; s – symmetric; u – stretching; α –deformation, δ - In plane bending; γ-out plane bending; τ – Twisting;

Table 1: FT-IR and FT-Raman experimental and calculated (scaled) vibrational frequencies of Bis(thiourea) Magnesium Sulphate (BTMS).

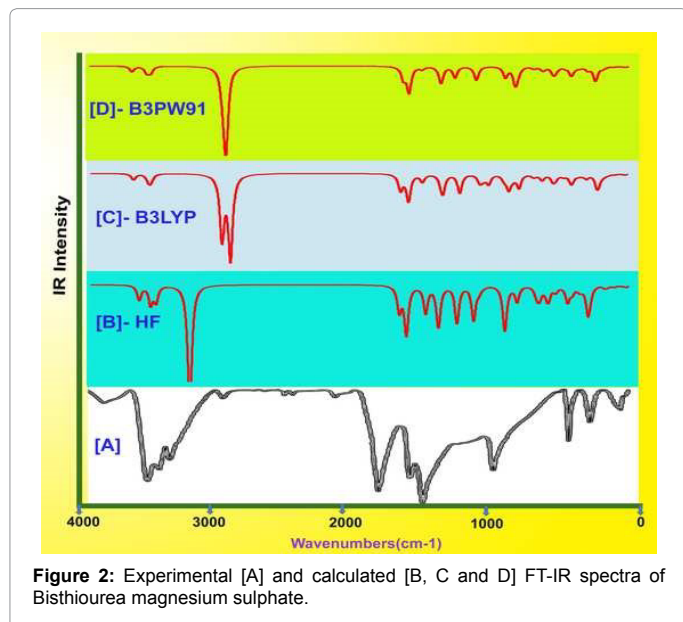


Figure 2: Experimental [A] and calculated [B, C and D] FT-IR spectra of Bisthiourea magnesium sulphate.

of the functional groups, GAUSSVIEW program and the calculated IR intensity and Raman activity etc.

N-H vibrations: The molecule consists of couple of NH₂ groups on both sides; there is a possibility of eight N-H stretching vibrations. In this present case, the N-H stretching frequencies are observed at 3773, 3755, 3381, 3296, 3277, 3192 and 3179 cm⁻¹. All the bands are assigned to symmetric vibrations. In addition to that, first two vibrational bands are found to be moved high from the expected region. This is mainly

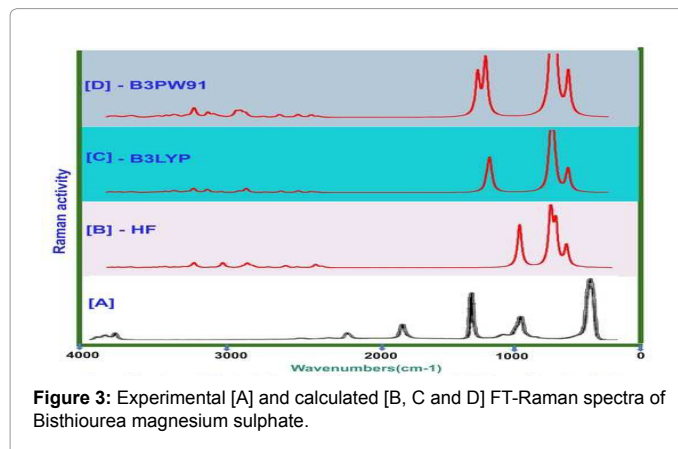


Figure 3: Experimental [A] and calculated [B, C and D] FT-Raman spectra of Bisthiourea magnesium sulphate.

due to the presence of sulphate with chain. The in-plane deformation vibrations for the present compound are observed at 1645, 1618, 1518, 1492, 1473, 1105, 1098 and 1083 cm⁻¹. The first two bands are moved up to the higher region and it is cleared that, these vibrations are favoured. The out-of-plane bending vibrations are set up at 960, 845, 715, 643, 625, 613, 590, 550, 545 and 520 cm⁻¹. Normally, whenever the metal atom coupled with the organic molecules, the normal vibrational modes of the same are suppressed much. From the N-H vibrations it is observed that, the entire out of plane vibrational modes are affected by other substitutions in the chain.

N=C=N vibrations: The symmetric N=C=N stretching vibrations occur in the region 2155-2130 cm⁻¹. The in the observed N=C=N stretching vibration was found at 2715, 2143, 2048 and 1836 cm⁻¹ IR spectrum and is due to greater double bond character of carbon to nitrogen on the formation of Mg [TU]₂ SO₄ complex.

C-N vibrations: In this present work, the C-N Stretching vibrations are observed at 1061, 998, 746, and 730 cm^{-1} which is making disagreement with the literature due to the loading of sulfur and metal atoms with the molecule. The C-NH₂ in-plane and out-of-plane bending vibrations are appeared at 510, 485, 230 and 210 & 200, 190, 155, 150 and 120 cm^{-1} respectively. These two vibrations are affected much by other vibrations which make disagreement with literature values (33-34) [9].

C-S vibrations: In this metal organic compound, the in-plane bending vibrations are found at 470 and 440 cm^{-1} and the out-of-plane

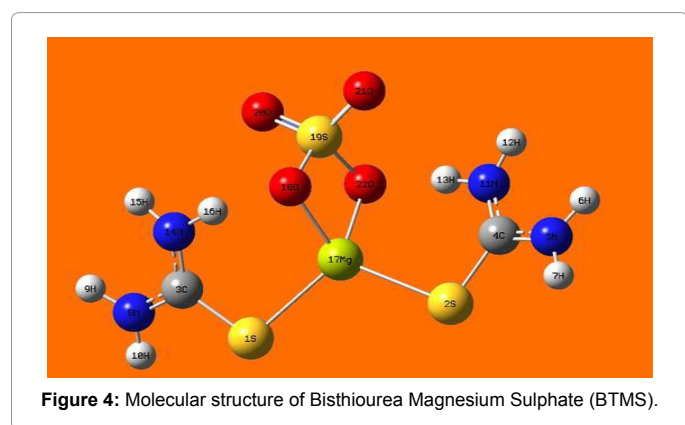
bending vibrations at 180, 160, 140, 130, 110, 105 and 100 cm^{-1} . These vibrational bands are pulled down to the lower region of the expected range due to the metal ion.

S=O vibrations: The symmetric S=O stretching vibrations occur in the region 1450-1350 cm^{-1} . The ν_1 in the observed IR and S=O stretching stretching vibration was found at 1412 and 1393 cm^{-1} Raman spectrum and is due to greater double bond character of sulfur to oxygen on the formation of Mg [TU]₂ SO₄ complex. This is mainly due to the presence of sulphate in the chain.

Mg-O-S vibrations: In BTMS, Mg-O-S stretching vibration was found at 435 and 425 cm^{-1} in IR spectrum. The in plane deformation vibrations for the present compound is observed at 422 and 390 cm^{-1} . The first two bands are moved up to the higher region and it is cleared that, these vibrations are favoured. The out of plane bending vibrations are set up at 340, 250 and 240 cm^{-1} . As all the IR bands have their counterparts in Raman suggests that the title crystal is non-centro symmetric.

Mulliken charge distribution analysis

The charge distribution on the molecule has an important influence on the vibrational spectra. The Mulliken charge levels of the molecule with different interactions were shown in Figure 5. The charge population was indicated in Table 4. Here, the negative charges are accumulated over the N atoms in thiourea even after the magnesium and sulphate ions are added. When the highly electronegative and



Geometrical Parameters	Methods				
	HF		B3LYP		B3PW91
	6-31++G (d-p)	6-311++G (d-p)	6-31++G (d-p)	6-311++G (d-p)	6-31++G (d-p)
Bond length(Å)					
(S1-C3)	1.7361	1.7341	1.7401	1.7391	1.7322
(S1-Mg17)	2.4885	2.4839	2.4765	2.4716	2.4702
(S2-C4)	1.7361	1.7341	1.7401	1.7382	1.7322
(S2-Mg17)	2.4885	2.484	2.4765	2.4666	2.4702
(C3-N8)	1.3296	1.3296	1.3461	1.3458	1.3432
(C3-N14)	1.3078	1.3071	1.3251	1.3224	1.3217
(C4-N5)	1.3296	1.3071	1.3461	1.3492	1.3432
(C4-N11)	1.3078	1.3296	1.3251	1.3203	1.3217
(N5-H6)	0.9946	0.9958	1.009	1.008	1.0078
(N5-H7)	0.9931	1.0101	1.007	1.0057	1.0061
(N8-H9)	0.9946	0.994	1.009	1.0078	1.0078
(N8-H10)	0.9931	0.9923	1.007	1.0058	1.0061
(N11-H12)	0.9963	0.994	1.0117	1.0108	1.0104
(N11-H13)	1.009	0.9923	1.0394	1.0416	1.0417
(N14-H15)	0.9963	0.9958	1.0117	1.0103	1.0104
(N14-H16)	1.009	1.0101	1.0394	1.0434	1.0417
(Mg17-O18)	1.9795	1.9849	1.9925	2.0136	1.993
(O18-S19)	1.5355	1.5322	1.5949	1.5887	1.5872
(S19-O20)	1.4372	1.4295	1.4686	1.4547	1.464
(S19-O21)	1.4372	1.4295	1.4686	1.4854	1.464
(S19-O22)	1.5356	1.5323	1.5949	1.558	1.5871

Bond angle(°)					
(C3-S1-Mg17)	103.4389	103.9473	101.0394	102.5485	100.9222
(C4-S2-Mg17)	103.4412	103.9441	101.0421	107.1544	100.9121
(S1-C3-N8)	117.1778	117.0547	117.0189	116.6413	116.9458
(S1-C3-N14)	123.8518	123.9383	123.8853	124.2817	123.786
(N8-C3-N14)	118.9564	118.9902	119.0762	119.0571	119.2487
(S2-C4-N5)	117.1763	123.9382	117.0185	115.8502	116.9488
(S2-C4-N11)	123.8531	117.055	123.8863	125.8269	123.7826
(N5-C4-N11)	118.9566	118.99	119.0756	118.2945	119.2491
(C4-N5-H6)	121.9032	120.5628	122.0381	121.9452	122.0782
(C4-N5-H7)	119.3295	121.0057	119.0765	118.8191	118.9961
(H6-N5-H7)	118.7575	116.6299	118.8713	118.627	118.9141
(C3-N8-H9)	121.9031	121.8539	122.039	122.1056	122.0789
(C3-N8-H10)	119.3296	119.2926	119.0746	119.1329	118.9952
(H9-N8-H10)	118.7573	118.8379	118.8715	118.7599	118.9132
(C4-N11-H12)	120.8345	121.8541	120.3358	119.2149	120.4376
(C4-N11-H13)	121.1151	119.2922	120.2831	126.2408	120.2488
(H12-N11-H13)	116.3764	118.8383	115.9381	114.0374	116.0717
(C3-N14-H15)	120.8348	120.5615	120.3366	120.3324	120.4368
(C3-N14-H16)	121.1141	121.0056	120.2829	121.2097	120.2506
(H15-N14-H16)	116.3742	116.6313	115.942	117.2738	116.077
(S1-Mg17-S2)	115.796	115.5599	115.3819	116.08	115.154
(S1-Mg17-O18)	105.12	104.301	104.9739	104.2932	104.7559
(S2-Mg17-O18)	126.8779	128.3368	126.4075	120.106	126.9659
(Mg17-O18-S19)	94.9933	95.5088	93.8543	92.1035	93.8338
(O18-S19-O20)	109.0452	109.0645	108.8066	110.6221	108.7984
(O18-S19-O21)	111.0894	111.157	110.7549	107.8245	110.6476
(O18-S19-O22)	98.2129	97.8249	97.9723	98.8904	98.2658
(O20-S19-O21)	116.7933	116.9201	117.9233	116.5139	117.9072
(O20-S19-O22)	111.0883	111.1565	110.7559	113.3861	110.6505
(O21-S19-O22)	109.0448	109.0659	108.8039	108.0517	108.7999
Dihedral angles(°)					
(Mg17-S1-C3-N8)	155.8392	156.3497	154.0423	160.5037	154.1954
(Mg 17-S1-C3-N14)	-25.5397	-25.1581	-27.5849	-21.1351	-27.4254
(C3-S1- Mg17-S2)	175.0829	173.6904	175.8918	160.245	176.4973
(C3-S1- Mg17-O18)	29.895	27.4397	32.0952	25.7374	32.3349
(Mg17-S2-C4-N5)	155.8526	-25.1612	154.0442	-152.2027	154.1519
(Mg17-S2-C4-N11)	-25.5238	156.3458	-27.5851	29.7805	-27.4747
(C4-S2- Mg17-S1)	175.0787	173.6918	175.8942	165.2823	176.5489
(C4-S2- Mg17-O18)	-48.4705	-49.6488	-49.2577	-67.7378	-48.5736
(S1-C3-N8-H9)	177.82	178.0341	174.8979	176.4153	174.9432
(S1-C3-N8-H10)	-3.3441	-3.4223	-3.6784	-4.0363	-3.745
(N14-C3-N8-H9)	-0.8713	-0.5357	-3.5564	-2.0357	-3.5129
(N14-C3-N8-H10)	177.9646	178.0078	177.8673	177.5127	177.7989
(S1-C3-N14-H15)	170.4248	170.7616	166.1288	172.682	166.5408

(S1-C3-N14-H16)	5.7163	6.5608	7.8969	5.4556	7.6536
(N8-C3-N14-H15)	-10.977	-10.7736	-15.5299	-8.9936	-15.1151
(N8-C3-N14-H16)	-175.6855	-174.9744	-173.7619	-176.2201	-174.0023
(S2-C4-N5-H6)	177.8161	170.7558	174.9173	-169.4895	174.9679
(S2-C4-N5-H7)	-3.3384	6.5548	-3.7001	1.4393	-3.7755
(N11-C4-N5-H6)	-0.8776	-10.7785	-3.5351	8.6844	-3.4827
(N11-C4-N5-H7)	177.968	-174.9796	177.8475	179.6133	177.7739
(S2-C4-N11-H12)	170.4263	178.0285	166.1201	-174.7373	166.534
(S2-C4-N11-H13)	5.7049	-3.4152	7.9029	-3.4179	7.6677
(N5-C4-N11-H12)	-10.9731	-0.5422	-15.5407	7.2896	-15.1278
(N5-C4-N11-H13)	-175.6945	178.0141	-173.7579	178.609	-173.994
(S1- Mg17-O18-S19)	-124.4391	-126.1082	-124.2745	-131.8945	-124.8501
(S2- Mg17-O18-S19)	95.5441	93.6065	97.2588	95.8735	96.7014
(Mg17-O18-S19-O20)	115.7481	115.6533	115.2054	130.3477	115.2052
(Mg17-O18-S19-O21)	-114.1429	-114.0016	-113.6402	-101.1879	-113.7522
(Mg17-O18-S19-O22)	0.0003	-0.0012	0.009	11.1305	-0.0025

Table 2: Optimized geometrical parameters for Bis(thiourea) Magnesium Sulphate (BTMS).

S. No	Observed frequency	Calculated frequency				
		HF		B3LYP		B3PW91
		6-31++G (d-p)	6-311++G (d-p)	6-31++G (d-p)	6-311++G (d-p)	6-31++G (d-p)
1	3773	3970	3949	3742	3721	3768
2	3755	3970	3949	3742	3720	3768
3	3381	3880	3858	3628	3611	3656
4	3296	3879	3857	3628	3603	3656
5	3277	3829	3814	3603	3591	3627
6	3192	3829	3814	3603	3588	3627
7	3179	3599	3549	3111	3055	3078
8	2715	3590	3539	3090	2992	3056
9	2143	1857	1854	1710	1713	1711
10	2048	1855	1852	1708	1711	1709
11	1836	1805	1797	1663	1655	1669
12	1645	1804	1796	1662	1652	1668
13	1618	1653	1643	1560	1549	1570
14	1518	1649	1639	1557	1546	1568
15	1492	1552	1543	1421	1408	1430
16	1473	1547	1538	1416	1393	1424
17	1412	1390	1389	1294	1268	1319
18	1393	1258	1254	1139	1127	1159
19	1105	1215	1210	1137	1113	1142
20	1098	1215	1210	1135	1087	1142
21	1083	1175	1173	1081	1078	1080
22	1061	1175	1173	1080	1051	1080
23	998	1016	1005	933	934	945
24	960	997	1000	925	900	937

25	845	899	904	843	870	863
26	746	897	904	821	823	843
27	730	756	756	711	714	723
28	715	753	752	705	706	718
29	643	736	736	656	652	660
30	625	729	722	656	644	660
31	613	727	720	645	643	646
32	590	668	671	576	580	583
33	550	647	652	564	566	570
34	545	600	595	552	555	555
35	520	600	594	551	545	554
36	510	581	582	536	536	538
37	485	512	514	487	488	491
38	470	508	508	480	488	483
39	440	504	498	439	440	442
40	435	501	497	438	433	441
41	425	463	464	433	427	437
42	422	458	459	432	423	434
43	390	453	455	403	410	406
44	340	406	407	376	378	376
45	250	390	388	368	350	368
46	240	360	334	314	314	315
47	230	359	333	243	237	256
48	210	320	315	242	226	255
49	200	212	213	207	211	208
50	190	192	198	200	195	201
51	180	171	174	181	175	182
52	160	169	172	168	155	166
53	155	123	123	119	118	117
54	150	108	107	114	109	114
55	140	105	104	112	99	111
56	130	86	87	86	82	85
57	120	59	56	54	63	54
58	110	53	52	51	54	50
59	105	30	25	33	33	33
60	100	23	21	22	21	22

Table 3: Calculated unscaled frequencies of Bis (thiourea) Magnesium Sulphate (BTMS).

positive atoms are coupled to formed dipoles, the remaining C and H of the molecule have positive space. Since the addition of magnesium sulphate have been occurred in thiourea, the sulphur atoms become low order negative that is almost neutral. Simultaneously, the chemical property has also changed for the same. This is the main cause for the compound was being optically active.

Single crystal XRD analysis

The lattice dimensions and the crystal system have been determined from the single X-ray diffraction analysis (Model: ENRAF NONIUS

CAD 4). The determined unit cell parameters and the observed crystal system are reported in the Table 5.

UV-Vis-NIR analysis

The Optical transmission spectra of BTMS was recorded using Varion Cary 5E UV- Vis-NIR spectro photometer in the range 200-2000 nm with high resolution and is shown in Figure 6. The crystal has a good transmission in the entire visible region. The low absorbance behaviour in the entire visible range also confirms colourless nature of the crystal. In the UV-Vis-NIR spectrum, the lower cut off is found

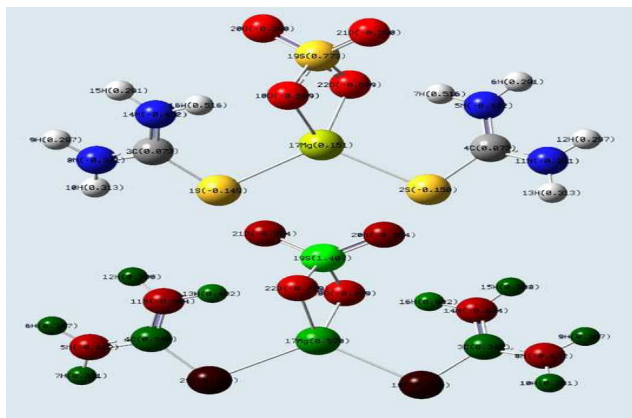


Figure 5: Mulliken charge (HF&DFT) of BTMS.

Atoms	HF / 6-311++G(d,p)	DFT-B3LYP / 6-311++G(d,p)
1S	- 0.149	- 0.176
2S	- 0.150	- 0.176
3C	0.073	0.348
4C	0.073	0.348
5N	-0.432	- 0.612
6H	0.291	0.307
7H	0.516	0.331
8N	- 0.371	- 0.612
9H	0.297	0.307
10H	0.313	0.331
11N	- 0.371	- 0.604
12H	0.297	0.308
13H	0.313	0.402
14N	- 0.432	- 0.604
15H	0.291	0.308
16H	0.516	0.402
17Mg	0.151	0.570
18O	- 0.609	- 0.729
19S	0.773	1.407
20O	- 0.390	- 0.564
21O	-0.390	- 0.564
22O	-0.609	- 0.729

Table 4: Mulliken atomic charge distribution of BTMS.

near 288 nm, which is an advantage in semi organic nonlinear optical materials over their inorganic counterparts [10].

Second Harmonic Generation (SHG) analysis

The second harmonic generation test was carried out by classical powder method developed by Kurtz and Perry. It is an important and popular tool to evaluate the conversion efficiency of NLO materials. The fundamental beam of 1064nm from Q switched Nd: YAG laser was used to test the second harmonic generation (SHG) property of pure BTMS crystals. Pulse energy 2.9mJ/pulse and pulse width 8ns with a repetition rate of 10Hz were used. The photo multiplier tube (Hamamatsu R2059) was used as detector and 90 degree geometry was employed. The input laser beam was passed through an IR detector and

then directed on the microcrystalline powdered sample packed in a capillary tube. The SHG signal generated in the sample was confirmed from the emission of green light from the sample [11]. Potassium dihydrogen orthophosphate (KDP) crushed into samples of identical size is used as reference material. The output of laser beam having the bright green emission of wavelength 532 nm confirms the second harmonic generation output as shown in Figure 7.

TGA/DTA analysis

The Thermogravimetric analysis and Differential thermal analysis (TGA and DTA) curves for BTMS were obtained using simultaneous thermogravimetric analyser (STA) at 409 °C (NET- ZSCH) made in Germany at a heating rate of 10 °C/min in Nitrogen were shown in Figure 8. The TGA curves shows that there was a weight loss of about 82.57% in the temperature range 243-289 °C. The weight loss in this range may be due to decomposition of Thiourea present in BTMS. The increase in decomposition temperature when compared to the decomposition temperature of thiourea which is 182 °C may be due to the formation of metal complex. This revealed the thermal stability of BTMS [12].

NMR analysis

The NMR spectral data was calculated at B3LYP method with 6-311++G(d,p) level on the basis of GIAO method and the chemical shifts of the compound are reported in ppm relative to TMS for ¹H and ¹³C NMR spectra which were presented in Table 6 and the corresponding spectra were shown in Figure 9. In the case of BTMS, the chemical shift of C3 and C4 are 190.34 and 197.05 ppm respectively. The chemical shift is same for C3 and C4 are both the carbons having similar groups. The chemical shift of both carbons is very high; it is also due to the migration of double bond from C-S to C-N. The chemical shift of H6, H7, H9, H10, H12, H13, H15 and H16 are 27.69, 26.93, 27.25, 26.48, 27.57, 27.28, 26.05 and 26.40 ppm respectively. From the entire chemical shift of the molecules it can be inferred that, the chemical property of the metal is directly mingled with organic molecules and

S. No.	Samples	a (Å)	b (Å)	c (Å)	α (°)	β (°)	γ (°)	Volume (Å ³)
1	Thiourea	14.82	8.90	7.86	90	90	90	1037.84
2	BTCC	5.80	13.07	6.48	90	90	90	491.22
3	BTZC	5.90	12.75	12.97	90	90	90	976.51
4	BTMS	5.50	7.66	8.56	90	90	90	361.38

Table 5: Lattice parameters of TU, BTCC, BTZC and BTMS.

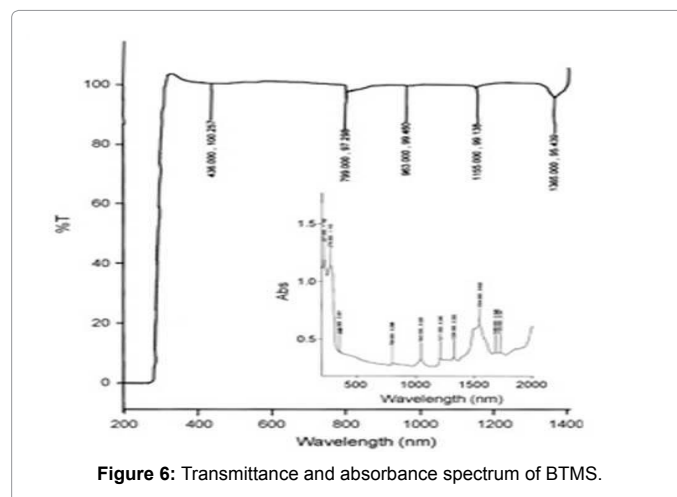


Figure 6: Transmittance and absorbance spectrum of BTMS.

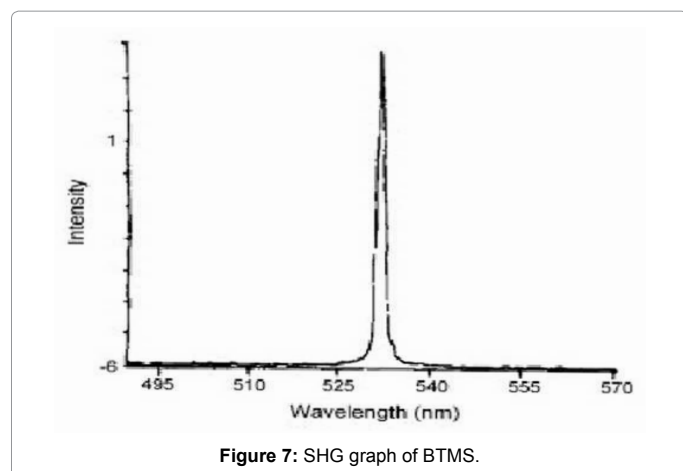


Figure 7: SHG graph of BTMS.

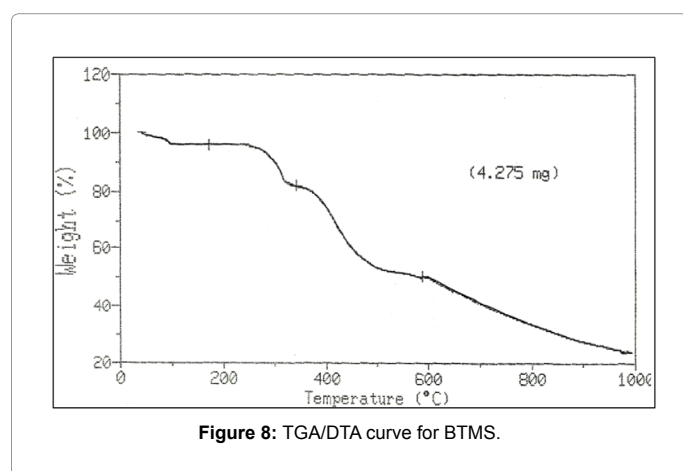


Figure 8: TGA/DTA curve for BTMS.

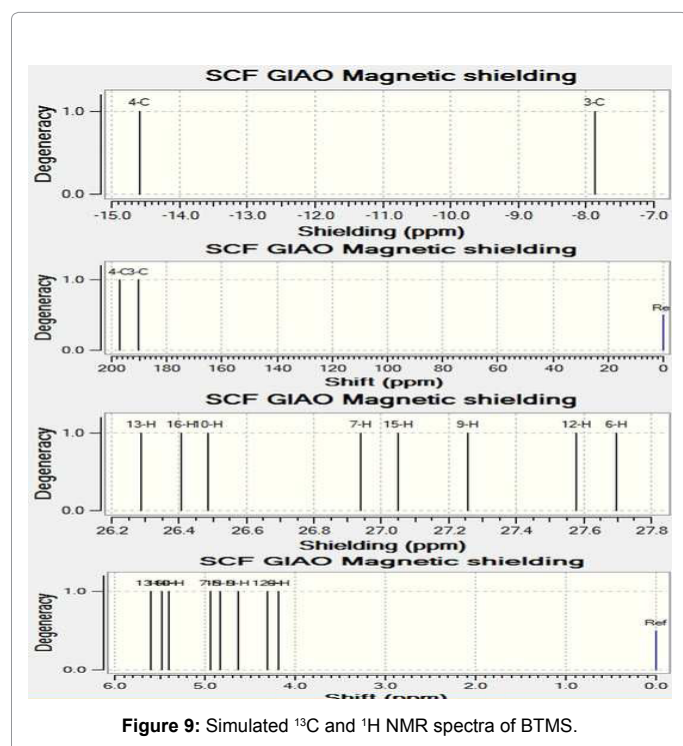


Figure 9: Simulated ^{13}C and ^1H NMR spectra of BTMS.

Atom	Theoretical			
	Gas	DMSO	Chloroform	CCl_4
H_6	27.69	26.76	27.02	27.27
H_7	26.93	26.58	26.71	26.80
H_9	27.25	26.52	26.67	26.86
H_{10}	26.48	26.08	26.15	26.25
H_{12}	27.57	26.67	26.88	27.12
H_{13}	27.28	26.16	26.12	26.14
H_{15}	26.05	26.59	26.68	26.80
H_{16}	26.40	26.43	26.48	26.47
C_3	190.34	188.34	188.64	189.29
C_4	197.05	190.47	192.08	197.77

Table 6: Calculated ^1H and ^{13}C NMR spectral data of BTMS.

this is the main cause for the present metal complex molecule having new chemical property.

Frontier molecular (electronic properties) analysis

The 3D diagram of the frontier molecular orbitals, in IR and UV-Visible region for title compound were displayed in Figures 10 and 11 respectively. According to such Figure, the HOMO is mainly localized over the magnesium, sulphate, N atoms and C-S group in which there are two sigma bond interaction taking place over the C-S of thiourea and one delta bond interaction over magnesium sulphate. From this observation, it is clear that, the in and out of phase interactions are present in HOMO and LUMO respectively. The electron transitions were happened between those HOMO and LUMO and thus the compound has been stabilized. During that time, the analogous physical and chemical properties mutually shared between the thiourea and magnesium sulphate. The charge levels were fluctuated due to the electron cloud sharing and were evidenced in the Mulliken charge analysis. The band gap of the present compound was found to be 5.61 eV.

Optical properties analysis

The electronic energy excitation of the present molecule were calculated at the B3LYP/6-311++G(d,p) level using the TD-DFT approach in gas phase and with the solvent of DMSO, Chloroform and CCl_4 . The calculated excitation energies, oscillator strength (f) and wavelength (λ) and spectral assignments are given in Table 7. The range of UV-Visible from 200 to 380 nm is the portion of the spectrum normally covered by the term ultraviolet. The compound under study is a semiconductor which was designed for the purpose of optoelectronic. In the solvent phases, there was no considerable disparity found. The molecular orbital lobe interaction in UV-Visible is appeared in Figure 11.

Molecular Electrostatic Potential (MEP) analysis

The colour code of these maps is in the range between -7.86 au (deepest red) to 7.86 au (deepest blue) in compound. The positive (blue) regions of MEP are related to electrophilic reactivity and the negative (green) regions to nucleophilic reactivity shown in Figure 12. As can be seen from the MEP map of the title molecule, the negative regions are mainly localized on nickel chloride and sulphur atoms. A maximum positive region is localized on the H of NH_2 groups indicating a possible site for nucleophilic attack. Though, this molecule contains different electron rich atoms, the negative potential regions located at metal combined atoms. From these results, it is found that, the metal atoms coupled strongly in the inertial position of organic lattice site.

λ (nm)	E (eV)	(f)	Major contribution	Assignment	Region	Bands
Gas						
853.02	1.4535	0.0004	H→L (86%)	$n \rightarrow \pi^*$	Quartz UV	B-band (German, radikalartig)
826.66	1.4998	0.0001	H→L+1 (85%)	$n \rightarrow \pi^*$		
804.60	1.5409	0.0028	H-1→L (78%)	$n \rightarrow \sigma^*$		
DMSO						
256.44	4.8348	0.0021	H→L (92%)	$n \rightarrow \sigma^*$	Quartz UV	B-band (German, radikalartig)
251.81	4.9237	0.0003	H-1→L (89%)	$n \rightarrow \sigma^*$		
244.99	5.0607	0.0580	H→L+1 (86%)	$n \rightarrow \sigma^*$		
Chloroform						
310.24	3.9964	0.0016	H-1→L+1 (83%)	$n \rightarrow \pi^*$	Quartz UV	B-band (German, radikalartig)
310.06	3.9987	0.0010	H→L+1 (92%)	$n \rightarrow \pi^*$		
292.87	4.2334	0.0016	H-1→L (89%)	$n \rightarrow \sigma^*$		
CCl₄						
406.66	3.0489	0.0004	H→L (86%)	$n \rightarrow \pi^*$	Quartz UV	B-band (German, radikalartig)
398.93	3.1079	0.0024	H→L+1 (85%)	$n \rightarrow \pi^*$		
380.87	3.2553	0.0009	H-1→L (78%)	$n \rightarrow \pi^*$		

Note: H: HOMO; L: LUMO

Table 7: Theoretical electronic absorption spectra of BTMS (absorption wavelength λ (nm), excitation energies E (eV) and oscillator strengths (f)) using TD-DFT/B3LYP/6-311++G(d,p) method.

Parameters	Values
HOMO	6.4000 eV
LUMO	0.7804 eV
Energy gap	5.6196 eV
Ionization potential (IP)	6.4000 eV
Electron affinity	0.7804 eV
Electrophilicity index (ω)	2.2936
Chemical potential (μ)	3.5902
Electronegativity (χ)	3.5902 eV
Chemical hardness (μ)	2.8098
Chemical softness (S)	0.1779
Dipole moment	4.8945 Debye

Table 8: Chemical parameters of BTMS.

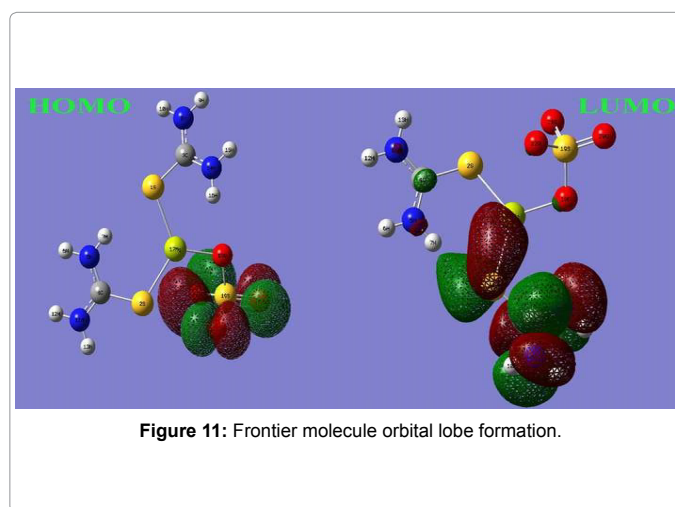


Figure 11: Frontier molecule orbital lobe formation.

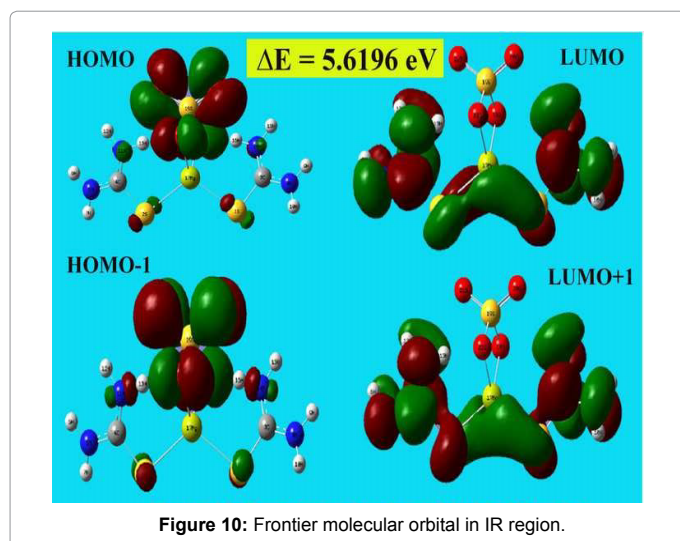


Figure 10: Frontier molecular orbital in IR region.

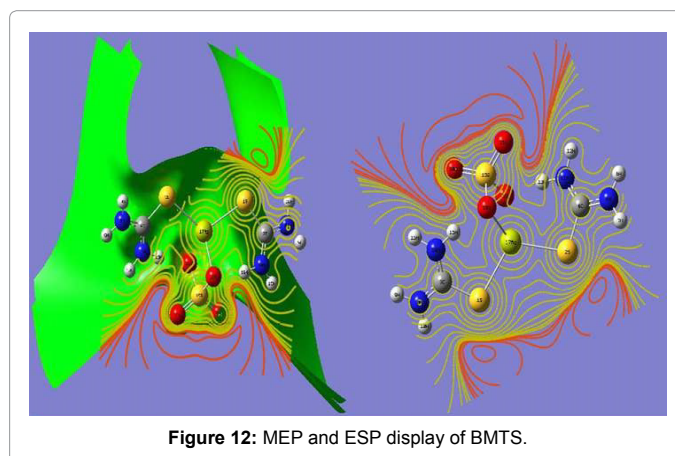


Figure 12: MEP and ESP display of BTMS.

Chemical properties

Usually, the chemical applications can be identified from the Chemical properties of the compounds. It is useful for recognizing the substance for the particular purpose. It was very important to know whether this compound is able to have rich potential for doping and starting material for semiconductor application. Accordingly, the chemical hardness and potential, electronegativity and Electrophilicity index were calculated and presented in Table 8. The dipole moment is another important electronic property of the chemical compound which is the ability of electrical and optical polarization of a substance. The large dipole moment leads the compound; very strong intermolecular interactions. The calculated dipole moment value for the present compound was 4.89 Debye. It was comparatively very high and the present molecule was being highly polar where the strong intermolecular interactions induced generally.

Conclusion

The FT-IR and FT-Raman spectra were recorded and the detailed vibrational assignments using HF and DFT methods with 6-31++G(d,p) and 6-311++G(d,p) basis sets were made for BTMS. The difference between the corresponding wave numbers (observed and calculated) is very small for most of fundamentals. Therefore, the results presented in this work for BTMS indicate that this level of theory is reliable for the prediction of both infrared and Raman spectra of the title compound. The equilibrium geometries of molecule have been determined and compared with X-ray analytical data. The optimization has been done in order to investigate the energetic behaviour and dipole moment of title compound in the gas phase and solvent. The electronic excitation in UV-VIS spectra was analysed. A reduction in absorption at Nd: YAG fundamental (1064 nm) observed in the optical transmission spectrum of BTMS recommends the crystal for nonlinear optical applications. The property of the second harmonic generation of the experimental crystal confirms the nonlinear nature of the crystal. The TGA/DTA curve recorded for the crystal confirmed its thermal stability.

References

1. Rosker MJ, Cunningham P, Ewbank MD, Marcy HO, Vachss FR, et al. (1996) Salt-based approach for frequency conversion materials. *Pure Appl Opt* 5: 667.
2. Selvasekarapandian S, Vivekanandan K, Kolaivaivel P, Gundurao TK (1997) Vibrational Studies of Bis (thiourea) Cadmium Chloride and Tris (thiourea) Zinc Sulphate Semiorganic Non-linear Optical Crystals. *Cryst Res Technol* 32: 299-309.
3. Min-hua J, Qi F (1999) Organic and semiorganic nonlinear optical materials. *Adv Mater* 11: 1147.
4. Chenthamarai S, Jayaraman D, Subramanian C, Ramasamy P (2001) Mechanical and optical studies on pure and nitro doped 4-hydroxyacetophenone. *Matter Lett* 47: 247.
5. Ramajothi J, Dhanushkodi S, Nagarajan K (2004) Crystal growth, thermal, optical and microhardness studies of tris (thiourea) zinc sulphate-a semiorganic NLO material. *Cryst Res Technol* 39: 414.
6. Meera K, Muralidharan R, Dhanasekaran R, Prapun M, Ramasamy P (2004) *J Cryst Growth* 263: 510.
7. Gunjan P, Joshi GC (2003) Second-order polarizabilities of some quinolines. *Indian J Pure Appl Phys* 41: 922-927.
8. Brahadeeswaran S, Venkataraman V, Sherwood JN, Bhat HL (1998) Crystal growth and characterization of semiorganic nonlinear optical material: sodium p-nitrophenolate dihydrate. *J Matter Chem* 8: 613-618.
9. Bellamy LJ, Williams RL (1957) The NH stretching frequencies of primary amines. *Spectrochimica Acta*, p: 341.
10. Krishnakumar V, Ramachandraraja C, Sundararajan RS (2007) Crystal growth and vibrational spectroscopic studies of the semiorganic non-linear optical crystal-bisthiourea magnesium sulphate. *Spectrochimica Acta Part A* 68: 113-116.
11. Hussaini SS, Dhumane NR, Dongre VG, Karmuse P, Ghughare P, et al. (2008) Effect of glycine on the optical properties of Zinc Thiourea Chloride (ZTC) single crystal. *Opt Elect Adv Mat Rapid Commun* 2: 108.
12. Lange NA (1976) Lange's Handbook of Chemistry. 11th edn. McGraw Hill, New Delhi, India.